Journal of the Mechanics and Physics of Solids 57 (2009) 1254–1266

Contents lists available at ScienceDirect

Journal of the Mechanics and Physics of Solids

journal homepage: www.elsevier.com/locate/jmps

Surface stress induced by interactions of adsorbates and its effect on deformation and frequency of microcantilever sensors

X. Yi [1], H.L. Duan *

State Key Laboratory for Turbulence and Complex System, Department of Mechanics and Aerospace Engineering, College of Engineering, Peking University, Beijing 100871, PR China

ARTICLE INFO

Article history:
Received 5 January 2009
Received in revised form
19 April 2009
Accepted 21 April 2009

Keywords:
Surface stress
Adsorption
van der Waals interaction
Coulomb interaction
Cantilever sensor

ABSTRACT

Surface stress is widely used to characterize the adsorption effect on the mechanical response of nanomaterials and nanodevices. However, quantitative relations between continuum-level descriptions of surface stress and molecular-level descriptions of adsorbate interactions are not well established. In this paper, we first obtain the relations between the adsorption-induced surface stress and the van der Waals and Coulomb interactions in terms of the physical and chemical interactions between adsorbates and solid surfaces. Then, we present a theoretical framework to predict the deflection and resonance frequencies of microcantilevers with the simultaneous effects of the eigenstrain, surface stress and adsorption mass. Finally, the adsorption-induced deflection and resonance frequency shift of microcantilevers are numerically analyzed for the van der Waals and Coulomb interactions. The present theoretical framework quantifies the mechanisms of the adsorption-induced surface stress, and thus provides guidelines to the analysis of the sensitivities, and the identification of the detected substance in the design and application of micro- and nanocantilever sensors.

1. Introduction

Surface stress has a great effect on the mechanical and physical properties of materials and devices, especially, nanomaterials and nanodevices (e.g., Kramer et al., 2004; Duan et al., 2005; Park and Klein, 2008). Since the bonding configurations of the atoms at surfaces become different when adsorbates are situated on the surfaces, surface stress can be altered by the presence of adsorbates. This mechanism constitutes the basis for chemical, physical and biological detections using cantilever sensors of micro- and nanosize. The most common methods to measure adsorption-induced change of surface stress are based on the static bending and the resonance frequency shift of vibration of microcantilever sensors. Generally, the bending of cantilevers is driven by an eigenstrain and the change of the surface stress (Stoney, 1909; Timoshenko, 1925; Freund, 1996; Li et al., 1999; Zang et al., 2007; Zang and Liu, 2008), while the vibration frequency shift is affected by the mass loading and surface elasticity (Gurtin et al., 1976; Ilic et al., 2000; Saya et al., 2004; Chun et al., 2007; Lachut and Sader, 2007; Park and Klein, 2008). Change of surface stress can arise from many interacting mechanisms of the adsorbates, including the electrostatic interaction, van der Waals (vdW) forces, dipole–dipole interaction and hydrogen bonding, changes in the charge distribution of surface atoms, and so on (Israelachvili, 1985; Grossmann et al., 1996; Berger et al., 1997; Chakarova-Käck et al., 2006; Sony et al., 2007). Experiments have revealed that the adsorption-induced surface

* Corresponding author. Tel.: +86 10 62753228; fax: +86 10 62751812.
E-mail address: hlduan@pku.edu.cn (H.L. Duan).
[1] Present address: The Division of Engineering, Brown University, Box D, 182 Hope Street, Providence, RI 02912, USA.

0022-5096/$ - see front matter © 2009 Elsevier Ltd. All rights reserved.
doi:10.1016/j.jmps.2009.04.010

stress results in the bending and resonance frequency shift of microcantilevers (Chen et al., 1995; Berger et al., 1997; Wu et al., 2001; McFarland et al., 2005; Hwang et al., 2006).

Extensive studies on surface stress induced by adsorbate interactions have been conducted by continuum approach, atomistic simulation and experiments (Kohn and Lau, 1976; Lau and Kohn, 1977; Berger et al., 1997; Pala and Liu, 2004). For example, Lau and Kohn (1977) investigated the indirect adsorbate interactions by treating an adsorbed atom as a force dipole on the surface of an unstrained half-space. Pala and Liu (2004) studied the effect of strain on the chemisorption energy based on the interaction energy between adsorbates and a solid surface. However, in these models, they only considered the indirect interactions between adsorbates mediated by the substrate and did not consider the direct adsorbate–adsorbate interactions. It is noted that as the density of adsorbates increases, the adsorbate–adsorbate interactions have to be considered. Generally, there are two kinds of adsorbate interactions: the physical interactions and chemical interactions. Among these, the van der Waals interaction is the major driving force for physisorption (Chakarova-Käck et al., 2006; Sony et al., 2007). For example, it is shown that the van der Waals interaction makes important contributions to the adsorption of thiophene on copper surfaces (Sony et al., 2007) and the adsorption of benzene and naphtalene on graphite (Chakarova-Käck et al., 2006). At present, although extensive studies have been carried out to gain insights into the adsorption problem, the quantitative relation between the adsorption-induced surface stress and the van der Waals interaction is not studied. Among the chemical interactions of adsorbates, the electrostatic interaction is important to the adsorption states of molecules with charging effects (Berger et al., 1997). For example, Berger et al. (1997) studied the adsorption-induced surface stress during the self-assembly of alkanethiols on gold by measuring the sensor deflection. McFarland et al. (2005) examined the influence of surface stresses induced by the adsorption of thiol molecules on the resonance frequency of a cantilever sensor. Chen et al. (1995) concluded that the resonance frequency shift of a cantilever can result from the change of both mass loading and spring constant induced by surface adsorption of chemicals. However, to the authors' knowledge, no relation is established between the adsorption-induced change of surface stress and the adsorbate interactions.

Therefore, at present, one big challenge in the development of microcantilever sensors is quantifying the connections between the properties of adsorbates and the adsorption-induced surface stress. As both the static deformation and the dynamic frequency are quantities at the continuum level, whereas the interactions exist at the atomic/molecular level, an effective way to addressing this challenge is to derive the continuum-level descriptions of the surface stress from the molecular-level descriptions of the adsorbate interactions. Based on the connection between the continuum-level and molecular-level descriptions, the static and dynamic response of cantilevers to adsorption can be analyzed. On the other hand, it was reported that the constant surface stress induced by molecular interactions affects the resonance frequency of microcantilevers (Lagowski et al., 1975; Chen et al., 1995; Hwang et al., 2006; Dorignac et al., 2006). However, Gurtin et al. (1976) showed that only the surface modulus results in the variation of resonance frequency. Therefore, it is important to develop a model to analyze the dynamic response of cantilevers to the surface modulus. A better understanding of the resonance behavior of cantilevers is essential to improve the design of sensors.

Due to the importance of the van der Waals interaction and electrostatic interaction in the interacting mechanisms of the adsorbates, in this paper, we first establish the connections between the surface stress at the continuum level and the adsorbate interactions (adsorbate–adsorbate interactions and adsorbate–surface interactions) at the molecular level for the van der Waals interaction and the Coulomb interaction. Then we analyze the static deformation and resonance frequency shift of two-layer cantilevers with the simultaneous effects of the eigenstrain, the surface stress and the adsorption mass. Finally, the adsorption-induced deflection and resonance frequency shift of microcantilevers are numerically analyzed based on the presented theoretical framework. Numerical results indicate that the effect of the surface stress and adsorption mass on the dynamic properties of cantilevers is crucial and depends on the type of the adsorbate and the interacting properties.

2. Surface stress due to vdW interaction

There exist interatomic/intermolecular forces between the adsorbates on a surface. Because the vdW interaction between the adsorbates is the major driving force for physisorption (Chakarova-Käck et al., 2006; Sony et al., 2007) and the electrostatic interaction is important to the adsorption states of molecules with charging effects (Berger et al., 1997), we investigate these two interactions in terms of the short-range Lennard-Jones (L-J) potential and the long-range Coulomb's law, respectively, and derive the relations between the surface stress at the continuum level and the adsorbate interactions at the atomic/molecular level.

Consider a cantilever with a thickness h and Young modulus E as shown in Fig. 1. For simplicity, we assume that the surfaces of the cantilever are chemically homogeneous, so the adsorbates are distributed statistically uniformly on the upper and lower surfaces, with the mean interspacing distance η between two adsorbates along the length direction as illustrated in Fig. 1. The origin of the coordinate system is on the geometrical midplane and the z-axis is perpendicular to the midplane. In this model, we also assume that the first layer of the adsorbates (adsorbates 2, 3, 5 and 6 in Fig. 1) on the cantilever surfaces play a dominant role and the effects of the second and higher layers of the adsorbates are less important (Dareing and Thundat, 2005; Huang et al., 2006).

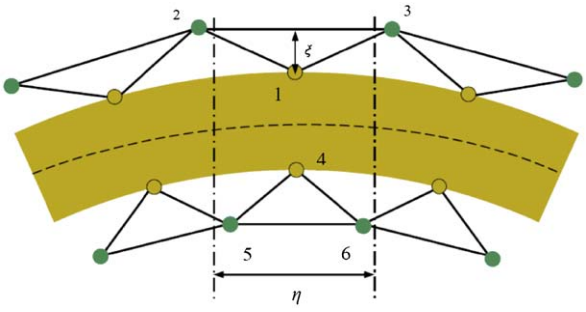

Fig. 1. A cantilever with a uniform distribution of atoms/molecules adsorbed both on the upper and lower surfaces.

Surface stresses τ_u and τ_l exist on the upper and lower surfaces of the cantilever, respectively. Here and in the following part, the subscripts u and l denote the quantities related to the upper and lower surfaces of the cantilever, respectively. Depending on the state of the elastic strain, τ can be expressed as (e.g., Gurtin and Murdoch, 1975)

$$\tau_u = a_u + b_u\varepsilon_u, \quad \tau_l = a_l + b_l\varepsilon_l, \tag{1}$$

where a denotes the constant (strain-independent) surface stress, b is the surface modulus, and ε_u and ε_l are the surface elastic strains. In particular, a constant surface stress $a>0$ means that the surface tends to contract and the surface is said to be in tension. On the contrary, $a<0$ indicates that the surface tends to expand and is said to be in compression. The strain-independent surface stress $a_{u(l)}$ and the surface modulus $b_{u(l)}$ can be expressed as

$$a_{u(l)} = a^0_{u(l)} + \Delta a_{u(l)}, \quad b_{u(l)} = b^0_{u(l)} + \Delta b_{u(l)}, \tag{2}$$

where the quantities with a superscript 0 denote the values before the adsorption, and Δ denotes the changes caused by the adsorption.

We first consider the vdW interaction based on the model used by Dareing and Thundat (2005) and Huang et al. (2006). The vdW interaction between the adsorbates (2, 3, 5 and 6) and the surfaces atoms (1 and 4), and that between the adsorbates themselves are depicted by the following Lennard-Jones (6-12-type) potential (cf. Fig. 1):

$$V(r_{ij}) = -\frac{A}{r_{ij}^6} + \frac{B}{r_{ij}^{12}}, \tag{3}$$

where r_{ij} is the distance between atoms i and j, and A and B are the Lennard-Jones constants. The distances between adjacent atoms are

$$\begin{aligned} r_{23} &= \eta\left[1+\varepsilon\left(\frac{h}{2}+\xi\right)\right], \quad r_{12} = r_{13} = \sqrt{\left(\frac{r_{23}}{2}\right)^2 + \xi^2}, \\ r_{56} &= \eta\left[1+\varepsilon\left(-\frac{h}{2}-\xi\right)\right], \quad r_{45} = r_{46} = \sqrt{\left(\frac{r_{56}}{2}\right)^2 + \xi^2}, \end{aligned} \tag{4}$$

where η is taken as the space between two adsorbates (the reciprocal of η is defined as the number density under the undeformed state (number per length), ξ is the distance between the adsorbates and surfaces (cf. Fig. 1), and $\varepsilon(h/2+\xi)$ and $\varepsilon(-h/2-\xi)$ are the values of the strains at $z=h/2+\xi$ and $z=-h/2-\xi$, respectively.

2.1. Strain-independent surface stress due to vdW interaction

We first establish the connection between the strain-independent surface stress a in Eq. (1) and the vdW interactions of the distributed adsorbates. Suppose that the adsorbates are only located on one surface of the cantilever (upper surface here) and there are only the surface stress a_u^0 and surface modulus b_u^0 on the upper surface before adsorption. According to Eq. (3), the potential due to the vdW interaction over the length L of the cantilever is

$$U_i(K) = \int_L \frac{\varrho}{\eta}[V(r_{12}) + V(r_{13}) + V(r_{23})]\,dx, \tag{5}$$

where ϱ is the number density under the undeformed state (number per width), $V(r_{12}) = V(r_{13}) = -A_1/r_{12}^6 + B_1/r_{12}^{12}$ and $V(r_{23}) = -A_2/r_{23}^6 + B_2/r_{23}^{12}$. K denotes the curvature. Here, A_1 and B_1 are L-J constants for the interaction between the adsorbates and the adjacent cantilever atoms, and A_2 and B_2 are L-J constants for two adjacent adsorbates. The elastic energy (U_{e1}) in the bulk and upper surface per unit width over the length L is

$$U_{e1}(K) = \frac{1}{2}\int_L \int_{-h/2}^{h/2} \sigma\varepsilon\,dx\,dz + \int_L \left(a_u^0\varepsilon_u + \frac{b_u^0}{2}\varepsilon_u^2\right)dx, \tag{6}$$

where $\sigma = E\varepsilon$, $\varepsilon = zK$. Here we assume that the extension of the cantilever is very small and makes little contribution to the deformation of the cantilever, which is always true when the thickness h is larger than 2 nm (Zang and Liu, 2007). Hence we neglect the extension of the cantilever in Eq. (6). The equilibrium state requires that the total potential energy $U_p(=U_i+U_{e1})$ should be stationary, namely, $\partial U_p/\partial K = 0$. With the modified Stoney formula $a_u = -(Eh^2+4hb_u)K/6$ (Zang and Liu, 2007), it follows that

$$\frac{a_u^0}{\varrho}+\frac{3(1+\zeta K)A_1}{\eta^7\left[\frac{1}{4}(1+\zeta K)^2+\left(\frac{\xi}{\eta}\right)^2\right]^4}+\frac{6A_2}{\eta^7(1+\zeta K)^7}-\frac{6(1+\zeta K)B_1}{\eta^{13}\left[\frac{1}{4}(1+\zeta K)^2+\left(\frac{\xi}{\eta}\right)^2\right]^7}-\frac{12B_2}{\eta^{13}(1+\zeta K)^{13}}=\frac{a_u}{\varrho}\left(\frac{3b_u^0+hE}{4b_u+hE}\right)\approx\frac{a_u}{\varrho}, \tag{7}$$

where $\zeta = h/2+\xi$. It is noted that if the extension of the cantilever is considered, the term $(3b_u^0+hE)$ on the right side of Eq. (7) should be $(4b_u^0+hE)$. Since b_u^0 and b_u are very small compared with hE when $h>2$ nm (Zang and Liu, 2007), $(3b_u^0+hE)/(4b_u+hE)\approx 1$, which yields Eq. (7). Under the condition $\zeta K \ll 1$, if we ignore ζK in the left-hand side of Eq. (7), then the relation between the adsorption-induced surface stress Δa_u and the interactions of the distributed adsorbates can be obtained

$$\Delta a_u = \frac{3\varrho}{\eta^7}\left(2A_2+\frac{A_1}{r_e^4}\right)-\frac{6\varrho}{\eta^{13}}\left(2B_2+\frac{B_1}{r_e^7}\right), \tag{8}$$

where $r_e = \frac{1}{4}+(\xi/\eta)^2$. It is observed that Δa_u increases linearly with increasing attractive constants A_1 and A_2, while decreases linearly with increasing repulsive constants B_1 and B_2. This is consistent with the properties of the surface stress, namely, a positive surface stress tends to contract the surface and a negative one expands the surface. Since A_1 and A_2 (B_1 and B_2) are usually in the same order and $\xi/\eta\approx 1$ when the density of adsorbates is high, from Eq. (8) we know that the adsorbate–adsorbate interaction (A_2, B_2) plays a more important role than the adsorbate–surface interaction (A_1, B_1) in the magnitude of the adsorption-induced surface stress.

2.2. Surface moduli due to vdW interaction

Next, we establish the relation between the vdW interactions of the adsorbates and the surface modulus b in Eq. (1). Suppose that the same adsorbates are located on both the upper and lower surfaces uniformly (cf. Fig. 1). The potential energy due to the vdW interaction over the length L is

$$U_i(K) = \int_L \frac{\varrho}{\eta}[2V(r_{12})+V(r_{23})+2V(r_{45})+V(r_{56})]\,dx = \int_L \frac{\varrho}{\eta}u_i\,dx, \tag{9}$$

where $V(r_{45}) = -A_1/r_{45}^6+B_1/r_{45}^{12}$ and $V(r_{56}) = -A_2/r_{56}^6+B_2/r_{56}^{12}$. The elastic energy ($U_{e2}$) in the bulk and upper and lower surfaces per unit width over L is

$$U_{e2}(K) = \frac{1}{2}\int_L\int_{-h/2}^{h/2}\sigma\varepsilon\,dx\,dz+\int_L\left[a^0(\varepsilon_u+\varepsilon_l)+\frac{b^0}{2}(\varepsilon_u^2+\varepsilon_l^2)\right]dx, \tag{10}$$

where $\sigma = E\varepsilon$, $\varepsilon = zK$. The kinetic energy of the adsorbates and the cantilever per unit width over L is

$$U_k(\dot w) = \frac{1}{2}\int_L\left(\rho h+\frac{2\varrho m_a}{\eta}\right)\dot w^2\,dx, \tag{11}$$

where ρ is the mass density of the cantilever, w is the deflection of the midplane, the overdot denotes the partial derivative with respect to time t, and m_a is the mass of each adsorbate. Introducing the Lagrangian function $L(w,\dot w,t) = U_k(\dot w)-U_i(K)-U_{e2}(K)$ into Hamilton's equation $\delta\int_{t_1}^{t_2}L\,dt = 0$ leads to

$$\frac{\partial^2}{\partial x^2}\frac{\partial}{\partial K}\left(\frac{Eh^3}{24}K^2+\frac{b^0h^2}{4}K^2+\frac{\varrho}{\eta}u_i\right)-\left(\rho h+\frac{2\varrho m_a}{\eta}\right)\frac{\partial^2 w}{\partial t^2} = 0. \tag{12}$$

By neglecting the extension of the cantilever, expanding $\partial u_i/\partial K$ into a Taylor series with respect to K, and keeping the first order term of K, the free vibration equation can be obtained from Eq. (12),

$$\left(\frac{Eh^3}{12}+\frac{b^0h^2}{2}+\frac{\varrho}{\eta}\frac{\partial^2 u_i}{\partial K^2}\bigg|_{K=0}\right)\frac{\partial^4 w}{\partial x^4}+\left(\rho h+\frac{2\varrho m_a}{\eta}\right)\frac{\partial^2 w}{\partial t^2} = 0. \tag{13}$$

Recall that the vibration equation in the bending mode is given by (see Appendix B)

$$TD'\frac{\partial^4 w}{\partial x^4}+(m+\Delta m)\frac{\partial^2 w}{\partial t^2} = 0, \tag{14}$$

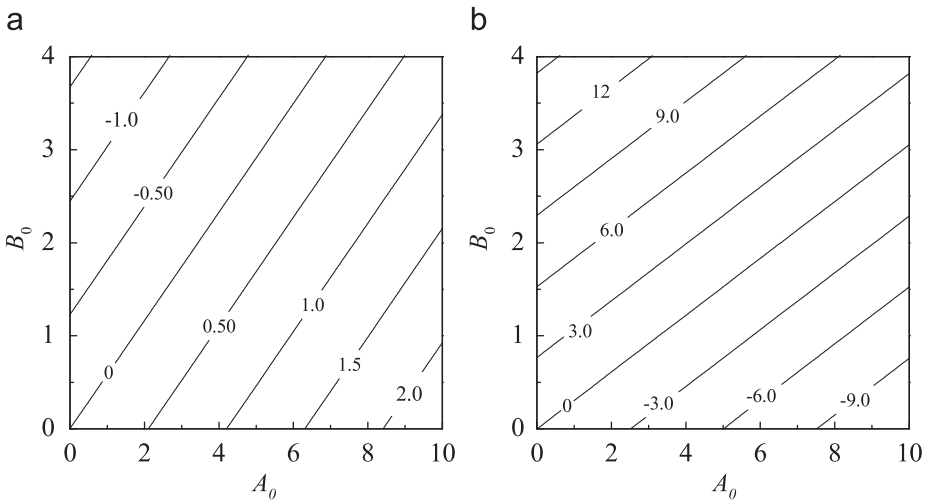

Fig. 2. Contours of $a\varrho^{-1}\times 10^9$ (a) and $b\varrho^{-1}\times 10^9$ (b) as functions of A_0 and B_0.

in which T is the width, m and Δm are the effective mass per unit length of the cantilever and the mass loading. Comparing Eq. (13) with the vibration equation (14), one obtains the bending stiffness per unit width D',

$$D' = \frac{Eh^3}{12} + \frac{b^0 h^2}{2} + \frac{\varrho}{\eta}\left.\frac{\partial^2 u_i}{\partial K^2}\right|_{K=0}, \tag{15}$$

where

$$\left.\frac{\partial^2 u_i}{\partial K^2}\right|_{K=0} = -\frac{3h^2}{2\eta^6}\left(14A_2 - \frac{A_1}{r_e^4} + \frac{2A_1}{r_e^5}\right) + \frac{3h^2}{2\eta^{12}}\left(52B_2 - \frac{2B_1}{r_e^7} + \frac{7B_1}{r_e^8}\right). \tag{16}$$

By letting Eq. (15) equal to $D' = Eh^3/12 + bh^2/2$ (Gurtin et al., 1976), the adsorption-induced surface modulus Δb is obtained

$$\Delta b = -\frac{3\varrho}{\eta^7}\left(14A_2 - \frac{A_1}{r_e^4} + \frac{2A_1}{r_e^5}\right) + \frac{3\varrho}{\eta^{13}}\left(52B_2 - \frac{2B_1}{r_e^7} + \frac{7B_1}{r_e^8}\right). \tag{17}$$

Note that Δb can be either positive or negative, depending on whether the repulsive interaction or the attractive one dominates. Similar to Eq. (8), the adsorbate–adsorbate interaction terms in Eq. (17) dominate the adsorption-induced surface modulus when the density of adsorbates is high. Both Eqs. (8) and (17) show that the adsorption-induced surface stress Δa and the surface modulus Δb are functions of the L-J constants (adsorption mechanism) and the location of adsorbates (surface coverage), and imply that the surface stress provides an insight into the adsorbate interactions as the density of adsorbates varies.

Next, we show some numerical results of the surface stress due to the vdW interaction. According to Eqs. (8) and (17), the contours of the change $\hat{a}(=\Delta a\varrho^{-1}\times 10^9)$ of the strain-independent surface stress, and the change $\hat{b}(=\Delta b\varrho^{-1}\times 10^9)$ of the surface modulus as functions of the normalized L-J constants A_0 and B_0 are shown in Figs. 2(a) and (b). We take $\xi = 0.282\,\text{nm}$ and $\eta = 0.324\,\text{nm}$ as have been used by Zhang et al. (2008), and the normalized L-J constants A_0 and B_0 are defined by $A_0^1 = A_0^2 \equiv A_0$ and $B_0^1 = B_0^2 \equiv B_0$ in which $A_1 = A_0^1\times 10^{-77}\,\text{J m}^6$, $A_2 = A_0^2\times 10^{-77}\,\text{J m}^6$, $B_1 = B_0^1\times 10^{-134}\,\text{J m}^{12}$ and $B_2 = B_0^2\times 10^{-134}\,\text{J m}^{12}$. The range of constants A_0 and B_0 considered in Fig. 2 are typical for different molecular structures, i.e., $A_0\in[0.02,10]$ and $B_0\in[0.02,4]$ (Rappé et al., 1992). If the number density ϱ is taken as the reciprocal of η ($\varrho = 1/\eta$), the constant surface stress change (Δa) induced by adsorption varies from about -4.5 to $6\,\text{N/m}$ ($\hat{a}$ varies from -1.5 to $2\,\text{N}$), as shown in Fig. 2(a). In the range of $A_0\in[0.02,0.15]$ and $B_0\in[0.02,0.15]$ which are the representative values of the adsorption of O atoms on a solid surface, the adsorption-induced surface stress is in the order of $0.1\,\text{N/m}$.

As shown in Fig. 2(b), the change of the adsorption-induced surface modulus Δb depicted by the L-J potential is about $1\,\text{N/m}$, which quantitatively agrees with the magnitude (-1 to $-0.1\,\text{N/m}$) of surface modulus in the paper of Lu et al. (2005). Once Δb is known, the frequency shift induced by the adsorption can be predicted by Eqs. (25) and (27) derived in Section 4. From Figs. 2(a) and (b), it is clear that when the attractive interaction dominates, a tensile constant surface stress and negative surface modulus are induced. The negative surface modulus will decrease the resonance frequency.

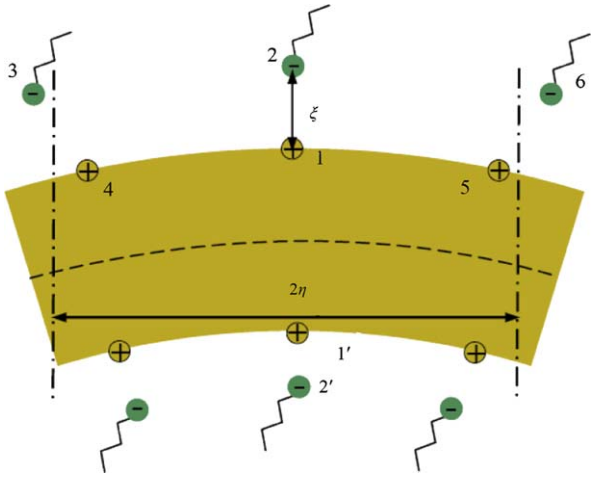

Fig. 3. Schematic illustration of adsorbates situated on the surface of a cantilever, where the alkanethiol molecules are adsorbed on the Au(111) surface.

3. Surface stress due to Coulomb interaction

Besides the vdW interaction, the Coulomb interaction is another important mechanism for the adsorption of small molecules and gas atoms, especially, when there exist charges or charge transfers in the considered system. It has been reported that the sulfur headgroup chemisorbs to the Au surface via the formation of Au–S bonds and the alkyl chains interact through the vdW attraction (Nuzzo et al., 1987). Though the vdW interaction between the alkyl chains results in the tilt of the chains, it has little contributions to the adsorption-induced surface stress (Berger et al., 1997; Godin, 2004). Moreover, Au–S bonds result in a partial charge transfer of approximately $0.3e$ between the Au and S atoms (Grönbeck et al., 2000). Due to the Coulomb interaction, the forces exerted between negatively charged sulfur headgroups and positively charged gold atoms contribute to the surface stress. To investigate the relation between the surface stress and the Coulomb interactions of adsorbates, we take the self-assembly of alkanethiols on the Au(111) surface in the vacuum condition as an example. The overlaying structure of alkanethiolates on the Au(111) surface can be described, using Wood's notation, as a $(\sqrt{3}\times\sqrt{3})R30^\circ$ overlayer of which a $c(4\times 2)$ superlattice can also be observed sometimes (Yourdshahyan and Rappe, 2002). Since the $(\sqrt{3}\times\sqrt{3})R30^\circ$ structure is the primary structure, our investigation is focused on it. For simplicity, we use the one-dimensional parallel configuration (see Fig. 3) to estimate the contribution of partial charge interactions to the surface stress, and this configuration can be extended to the case of $c(4\times 2)$ superlattice. In this model, the partial charge transfer at the Au–S bond is treated as two point charges (Godin, 2004). As depicted in Fig. 3, the adsorbates (2, 3, 6 and 2′) are partially negatively charged sulfur headgroups while the surface atoms (1, 4, 5 and 1′) are positively charged gold atoms.

The electrostatic energy, $W(r_{jk})$, for the Coulomb interaction between two electric charges is given by

$$W(r_{jk}) = \frac{1}{4\pi\varepsilon_0}\frac{q_j q_k}{r_{jk}}, \tag{18}$$

where r_{jk} is the distance between charges j and k, $q(=eZ)$ is the electric charge of the corresponding particle, $e(=1.602\times 10^{-19}\,\mathrm{C})$ is the elementary charge and Z is the ionic valency, and $\varepsilon_0(=8.8542\times 10^{-12}\,\mathrm{C^2/N\,m^2})$ denotes the permittivity of free space. For the like charges, $W(r_{jk})$ is positive, while for the unlike charges it is negative. The long-range Coulomb energy for a system of N charges is given by $W=\sum_{j=1}^{N} W_j$, where W_j is the electrostatic interaction energy of the charge j with all the other charges, and can be expressed as

$$W_j = \frac{1}{2}\times\frac{1}{4\pi\varepsilon_0}\sum_{k=1,k\neq j}^{N}\frac{q_j q_k}{r_{jk}}. \tag{19}$$

Similar to Eq. (5), if the adsorbates are only located on the upper surface, the potential $U_i(=\varrho(W_1+W_2))$ due to the Coulomb interaction over the length η is

$$U_i = \frac{\varrho q^2}{8\pi\varepsilon_0}\sum_{n=1}^{\infty}\left(\frac{2}{nr_{14}}+\frac{2}{nr_{23}}-\frac{2}{\sqrt{r_{14}^2n^2+\xi^2}}-\frac{2}{\sqrt{r_{23}^2n^2+\xi^2}}-\frac{2}{\xi}\right), \tag{20}$$

where W_1 and W_2 are the electrostatic interaction energies of the Au atom (atom 1) and the sulfur headgroup (adsorbate 2, cf., Eq. (19)). $r_{14}=\eta[1+\varepsilon(h/2)]$, r_{23} is given in Eq. (4), and ξ is the distance between the sulfur headgroup and the gold surface.

With the elastic energy U_{e1} in Eq. (6) and the Coulomb interaction in Eq. (20), the total energy is $U_p = U_i + U_{e1}$. From the relation $\partial U_p/\partial K = 0$ and following the similar procedure as shown in Section 2.1, we obtain the expression of the change Δa of the strain-independent surface stress due to the electrostatic interaction,

$$\Delta a = \frac{\varrho q^2}{2\pi\varepsilon_0\eta^2}\sum_{n=1}^{\infty}\frac{1}{n}\left[-1+\left(1+\frac{\xi^2}{\eta^2 n^2}\right)^{-3/2}\right], \tag{21}$$

where η is the distance between adjacent adsorbates (sulfur headgroups) under the undeformed state.

When the same adsorbates are situated on the two surfaces of the cantilever, the potential energy due to the Coulomb interaction over the length η is $U_i = \varrho(W_1 + W_2 + W_{1'} + W_{2'})$, where W_j ($j = 1, 2, 1', 2'$) is given in Eq. (19). Using Hamilton's equation, the elastic energy and kinetic energies (cf. Eqs. (10) and (11)), and following the procedure in Section 2.2, the surface modulus change Δb can be obtained:

$$\Delta b = \frac{\varrho q^2}{2\pi\varepsilon_0\eta^2}\sum_{n=1}^{\infty}\frac{1}{n}\left[2-3\left(1+\frac{\xi^2}{\eta^2 n^2}\right)^{-5/2}+\left(1+\frac{\xi^2}{\eta^2 n^2}\right)^{-3/2}\right]. \tag{22}$$

Due to the Coulomb interactions between the charged Au atoms and S headgroups, the adsorption of alkanethiols on the Au(111) surface results in the surface stress. The charge transfer from Au to S is about $q = 0.3e$ for the adsorption of thiols (Grönbeck et al., 2000), the distance between the sulfur headgroups and Au(111) surface is approximately 0.2 nm (Yourdshahyan and Rappe, 2002), the distance η between adjacent sulfur headgroups is about $\sqrt{3}a_{\mathrm{Au}}$, and the number density (ϱ) of sulfur headgroups is about $2/(3a_{\mathrm{Au}})$ (the lattice constant of Au is $a_{\mathrm{Au}} = 2.884$ Å). According to Eq. (21), the change of the strain-independent surface stress due to the adsorption of thiols on the Au(111) surface is $\Delta a = -0.095$ N/m, which is in the order of 0.011–0.019 N/m in the experiment done by Berger et al. (1997). From Eq. (21), the change of the surface modulus due to the adsorption of thiols on the Au(111) surface is $\Delta b = 0.3522$ N/m.

4. Mechanics of microcantilevers based on adsorption-induced surface stress

4.1. Static and dynamic properties

To investigate the impact of the adsorption-induced surface stress on the static and dynamic properties of microcantilevers, we consider a classical thin film/substrate structure shown in Fig. 4, which has a wide range of applications as microelectromechanical components (Berger et al., 1997; Li et al., 1999; Wu et al., 2001; Kramer et al., 2004). The thickness and Young modulus of the film (upper layer) are h_f and E_f, respectively, and those of the substrate (lower layer) are h_s and E_s. A perfect bonding is assumed between the two layers. The coordinate system is defined such that the interface of the film and substrate is located at $z = 0$, and the upper and lower surfaces are located at $z = h_f$ and $z = -h_s$, respectively. In the film, there is an eigenstrain $\varepsilon^*(z)$ as a function of coordinate z. The eigenstrain denotes the mismatch strain that may arise from the different lattice constants and/or the hygro-thermal expansion coefficients between the film and the substrate. We regard the two surfaces and two bulk layers as a whole system; hence the surface stress τ and the bulk stress in the cross-section are in equilibrium.

We first analyze the deformation of the two-layer cantilever due to the eigenstrain ε^* and the surface stress τ simultaneously. The detailed process to derive the static deformation is given in Appendix A. According to the equilibrium equations of the cantilever, i.e., the zero resultant forces due to the uniform strain and bending strain components, and the zero bending moment, the curvature K due to the eigenstrain and the surface stress can be obtained:

$$K = \frac{6E_f\int_0^{h_f}(z-h_b)\varepsilon^* dz + 6(h_f-h_b)b_u\varepsilon^*(h_f) + 3c_0h_fh_b(E_f+E_s) + 3\Gamma_1}{6(h_s+h_b)^2b_l + 6(h_f-h_b)^2b_u + 2\Gamma_2}, \tag{23}$$

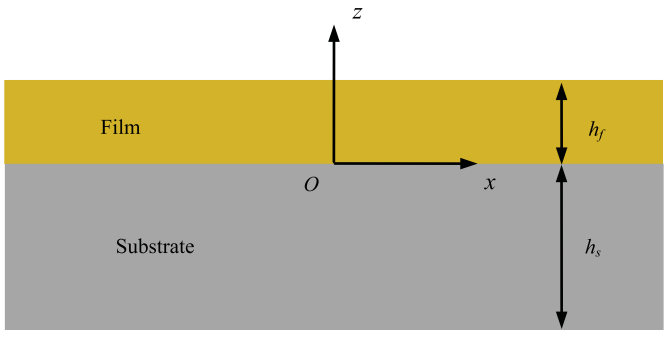

Fig. 4. Schematic diagram of a two-layer cantilever.

where

$$\Gamma_1 = (h_s + h_b)(2a_l + 2c_0 b_l + c_0 h_s E_s) - (h_f - h_b)(2a_u + 2c_0 b_u + c_0 h_f E_f),$$
$$\Gamma_2 = h_f(h_f^2 - 3h_f h_b + 3h_b^2)E_f + h_s(h_s^2 + 3h_s h_b + 3h_b^2)E_s, \tag{24}$$

$\varepsilon^*(h_f)$ denotes the eigenstrain at $z = h_f$, and c_0 and h_b are given in Eqs. (A.6) and (A.7). Non-uniform eigenstrain can be used to simulate the strain relaxation which is important to the growth of strained islands and thin films (Freund, 1996; Huang et al., 2005). If the eigenstrain is uniform, Eq. (24) reduces to a modified Timoshenko formula (Eq. (9) in the paper of Zang and Liu, 2008), which is obtained by the scheme of the strain energy minimization. In Eq. (23), the assumption in the classical Stoney (1909) formula that the film thickness is much less than that of the substrate ($h_f/h_s \ll 1$) is abandoned. Under the condition $h_f/h_s \ll 1$ and a constant eigenstrain (or a constant surface stress), Eq. (23) reduces to the classical Stoney formula. Eq. (23) can be regarded as a generalized Stoney formula.

Next, we analyze the dynamic property of the two-layer cantilever taking into account the surface modulus and the adsorption mass simultaneously. The bending stiffness per unit width, D', of the two-layer cantilever in the vibration equation as depicted in Eq. (14) is

$$D' = \frac{E_f h_f + 4b_u}{12\Gamma_3}[E_s h_s(3h_f^2 + 3h_f h_s + h_s^2) + E_f h_f^3] + \frac{(h_f + h_s)^2 b_u b_l}{\Gamma_3} + \frac{E_s h_s + 4b_l}{12\Gamma_3}[E_f h_f(h_f^2 + 3h_f h_s + 3h_s^2) + E_s h_s^3], \tag{25}$$

where $\Gamma_3 = b_u + b_l + h_f E_f + h_s E_s$. The details of the derivation for Eq. (25) are given in Appendix B. The solution to Eq. (14) gives the resonance frequency ($\tilde{f}_i$) of the ith mode of the cantilever clamped on one end with the effects of the changes of the mass and stiffness,

$$\tilde{f}_i = \frac{1}{2\pi}\left(\frac{\lambda_i}{L}\right)^2 \sqrt{\frac{T(D + \Delta D)}{m + \Delta m}}, \tag{26}$$

where L denotes the length of cantilever, λ_i represents the eigenvalue of the equation $\cos\lambda_i \cosh\lambda_i + 1 = 0$, $\Delta D(= D' - D)$ is the change of the bending stiffness, and D is given in Eq. (25) by letting $b_u = b_l = 0$. If $\Delta D = \Delta m = 0$, Eq. (26) reduces to the resonance frequency f_i without the mass loading and the change of bending stiffness.

If $\Delta D \ll D$ and $\Delta m \ll m$, the frequency shift ($\Delta f_i = \tilde{f}_i - f_i$) is

$$\Delta f_i \approx \frac{1}{4\pi}\left(\frac{\lambda_i}{L}\right)^2 \sqrt{\frac{T}{m}}\left(\frac{\Delta D}{D} - \frac{\Delta m}{m}\right). \tag{27}$$

Eqs. (14) and (27) show that the frequency shift is determined by a combination of the mass loading and the change of the bending stiffness, while the eigenstrain $\varepsilon^*(z)$ and the strain-independent surface stress a do not influence the resonance frequency. Similar phenomena exist in the thermoelastic problem of microscale beam resonators (Sun et al., 2006). Based on the dynamic characteristics of the cantilevers with the surface stress and mass loading, the cantilever sensors can be divided into three categories: (I) mass sensors, whose dynamic response is influenced by the adsorbed mass, and its frequency shift is $\Delta f_i^{(m)} = -\Delta m/2mf_i$; (II) surface stress sensors, whose dynamic response is influenced by the surface modulus, and the corresponding frequency shift is $\Delta f_i^{(s)} = \Delta D/2Df_i$; (III) mass and surface stress sensors, whose dynamic response is influenced by the two factors simultaneously, and the frequency shift is $\Delta f_i = \Delta f_i^{(m)} + \Delta f_i^{(s)}$ depicted by Eqs. (25) and (27). For example, Chen et al. (1995) showed by experiments that both the adsorbed mass and surface stress affect the resonance frequency of a gelatin-coated cantilever when it is exposed to water vapor.

From the expressions of $\Delta f_i^{(s)}$, we can conclude that the frequency shift $\Delta f_i^{(s)}/f_i$ increases with the increase of the surface modulus and decreases with the increase of the thickness and the Young moduli of the bulk layers. If $E_f = E_s = E$, $h = h_s + h_f$ and $b_l = 0$, $\Delta f_i^{(s)}$ can be particularly expressed as

$$\frac{\Delta f_i^{(s)}}{f_i} = \frac{3}{2\left(1 + \dfrac{hE}{b_u}\right)}. \tag{28}$$

For this case, $\Delta f_i^{(s)}/f_i$ is a function of a non-dimensional parameter hE/b_u.

As indicated in Eqs. (25) and (27), for surface stress sensors and mass and surface stress sensors, the strain-independent surface stress a does not change the resonance frequency. This conclusion is different from some results in the literature. In some models, the dynamic analysis of the cantilever is conducted on the bulk layer, while the surface stress a is simply expressed as an equivalent external axial force $(a_u + a_l)T$ (Lagowski et al., 1975; Saya et al., 2004) or $(a_u + a_l)L$ (Chen et al., 1995; McFarland et al., 2005; Dorignac et al., 2006; Hwang et al., 2006). However, as made clear by Gurtin et al. (1976), the distributed loading $q = (a_u + a_l)T\partial^2 w/\partial x^2$ by the surface stress cancels the effect of the equivalent external axial force on the resonance frequency. Hence, the strain-independent surface stress has no effect on the frequency shift (Gurtin et al., 1976), which is shown in Eqs. (25) and (27). In the sequel, the application of the theoretical framework in Sections 2 and 3 to the composite cantilever sensor shown in Fig. 4 is demonstrated in detail by some examples.

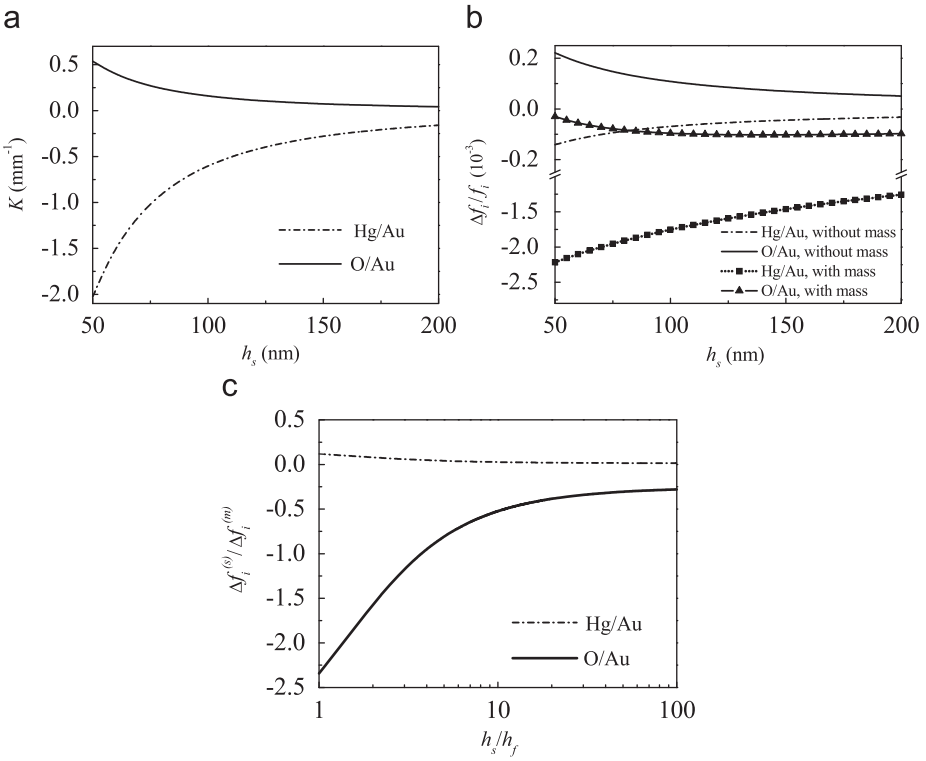

Fig. 5. Variations of the bending curvature (a) and normalized frequency shift (b) with substrate thickness h_s due to the vdW interaction; (c) ratio of frequency shifts due to surface stress ($\Delta f_i^{(s)}$) and mass loading ($\Delta f_i^{(m)}$) verse normalized substrate thickness.

4.2. Numerical results

The curvature and normalized frequency shift of a cantilever consisting of a Si substrate and a Au film due to the vdW interaction of adsorbates are plotted in Figs. 5(a) and (b). The parameters of the cantilever are: $E_s = 180\,\text{GPa}$, $\rho_s = 2.33\,\text{g/cm}^3$, $E_f = 90\,\text{GPa}$, $h_f = 20\,\text{nm}$, $\rho_f = 19.3\,\text{g/cm}^3$. Two cases are considered, namely, mercury (Hg) atoms on Au(1 0 0) with $A_0^1 = A_0^2 = 2.8377$, $B_0^1 = B_0^2 = 1.943$, $\xi = 0.45\,\text{nm}$, $\eta = 0.4\,\text{nm}$ (Dareing and Thundat, 2005); oxygen (O) atoms on Au(1 0 0) surface with $A_0^1 = 0.103$, $B_0^1 = 0.07885$, $A_0^2 = 0.1534$, $B_0^2 = 0.141$, $\xi = 0.282\,\text{nm}$, $\eta = 0.324\,\text{nm}$ (A_0^1, A_0^2, B_0^1 and B_0^2 are defined in Section 2) (Rappé et al., 1992; Zhang et al., 2008). The mass of a Hg atom is $m_a = 201\text{Da}$ and that of an oxygen atom is $m_a = 16\text{Da}$ (where $1\text{Da} = 1.66 \times 10^{-27}\text{kg}$). According to Eqs. (8), (17), (27) and (A.10), the bending curvature K and the normalized frequency shift $\Delta f_i/f_i$ as functions of the thickness of substrate are shown in Figs. 5(a) and (b). Here we assume that the surface stresses on the upper and lower surfaces are zero before adsorption, taking $\varrho = \eta^{-1}$ and $\Delta m/m = m_a/[\eta^2(\rho_f h_f + \rho_s h_s)]$. As shown in Figs. 5(a) and (b), for the adsorption of mercury vapor on gold surface, $K < 0$ and $\Delta f_i/f_i < 0$ without the consideration of mass loading effect, indicating that the adsorption-induced surface stress a is positive, whereas the surface modulus b is negative. For the case of O/Au(1 0 0), the adsorption-induced surface stress a is negative but the surface modulus b is positive. It is seen that K increases as the thickness h_s decreases. With consideration of the atom mass, $\Delta f_i/f_i$ changes significantly after the adsorption of Hg or O atoms on gold surface as shown in Fig. 5(b), which indicates that the mass of the adsorbates plays an important role in changing the resonant frequency besides the adsorbate interactions. To elucidate the effects of mass and surface modulus clearly, Fig. 5(c) shows the ratio $\Delta f_i^{(s)}/\Delta f_i^{(m)}$, namely, the ratio of the frequency shift $\Delta f_i^{(s)}$ due to the surface modulus to that $\Delta f_i^{(m)}$ due to the mass, as a function of h_s/h_f. It is seen that the ratio $\Delta f_i^{(s)}/\Delta f_i^{(m)}$ depends on the type of the adsorbate and the interacting properties. For example, in the case of O/Au(1 0 0), the influence of the adsorption-induced surface modulus on Δf_i is larger than that of the mass on Δf_i under $h_s < 4h_f$. As h_s becomes large, $\Delta f_i^{(s)}/\Delta f_i^{(m)}$ reaches a value about -0.5, suggesting that the effects of the mass and the adsorbate interactions are comparably important even for large h_s/h_f. For the Hg/Au(1 0 0) system, the mass loading effect dominates the frequency shift and the influence of Hg atom interactions can be neglected.

For the Coulomb interaction, we consider butanethiol molecules adsorbed on the gold surface of the cantilever in Fig. 4. The variations of K and $\Delta f_i/f_i$ with the space η of adsorbates for $q = 0.3e$ is shown in Figs. 6(a) and (b). The cantilever parameters are the same as those used for the vdW interaction in Fig. 5, except $h_s = 200\,\text{nm}$. The mass of a butanethiol molecule, m_a, is about 89Da, and $\Delta m/m = \varrho m_a/[\eta(\rho_f h_f + \rho_s h_s)]$. As shown in Figs. 6(a) and (b), the curvature K and the normalized frequency shift $\Delta f_i/f_i$ decrease with the increase of the adsorbate space η, indicating that the number density of adsorbates has a significant effect on the static and dynamic properties of cantilever sensors. As the number density ϱ

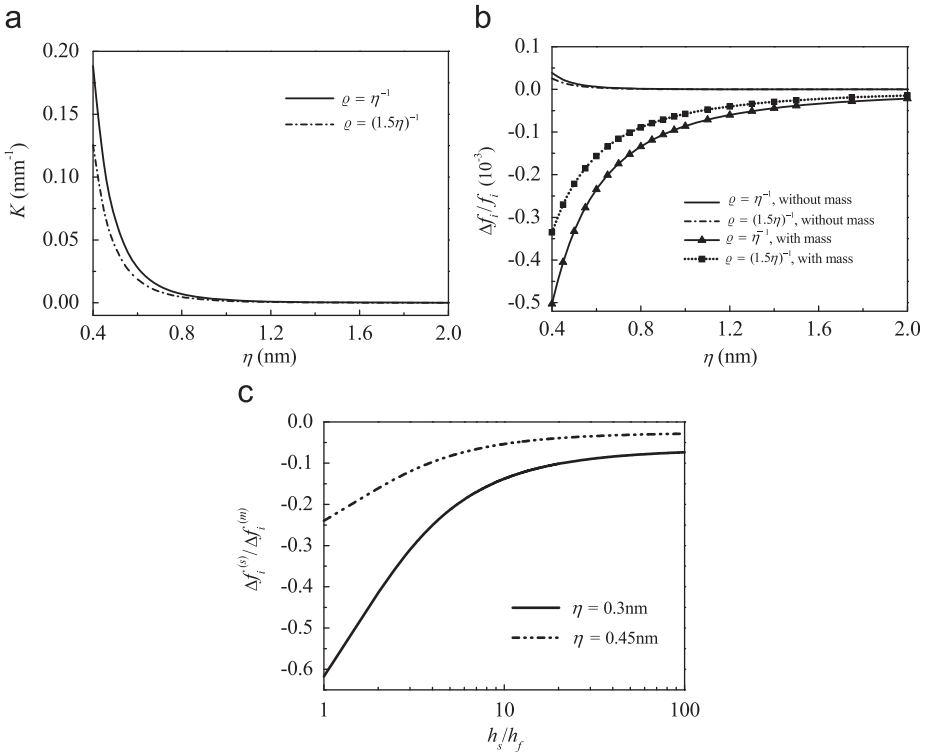

Fig. 6. Variations of the curvature (a) and normalized frequency shift (b) with adsorbate space η for a two-layer cantilever due to the Coulomb interaction between the adsorbates; (c) ratio of frequency shifts due to surface stress ($\Delta f_i^{(s)}$) and mass loading ($\Delta f_i^{(m)}$) as a function of h_s/h_f.

increases, the bending curvature and resonance frequency shift become large. $K>0$ and $\Delta f_i/f_i>0$ without the consideration of mass loading effect indicate that the adsorption-induced surface stress a is negative and the surface modulus b is positive. In Fig. 6(b), we can see that although the Coulomb interaction has an influence on the resonance frequency shift, the large resonance frequency shift comes from the mass of the adsorbates. Fig. 6(c) illustrates the dependence of ratio $\Delta f_i^{(s)}/\Delta f_i^{(m)}$ on h_s/h_f for $\eta=0.3$ and 0.45 nm. It is seen that for the case of low density of adsorbates ($\eta=0.45$ nm), the mass effect dominates the dynamic properties of cantilevers. For the high density of adsorbates ($\eta=0.3$ nm), the surface modulus resulting from the adsorbate interactions contributes a lot to the frequency shift, especially for a small h_s/h_f.

5. Conclusions

The connection between the surface stress in the continuum level and the adsorbate interactions in the molecular level, including the van der Waals interaction and Coulomb interaction, is established by considering the interaction energy, the elastic energy and kinetic energy of a cantilever. Then a theoretical framework is presented to analyze the deflection and resonance frequency of a two-layer cantilever due to the eigenstrain, surface stress and adsorption mass, simultaneously. The mass and number density of adsorbates, the cantilever size and the adsorption mechanism play an important role in the variations of the bending curvature and resonance frequency of cantilevers. The magnitude of resonance frequency shift due to the mass loading and the surface modulus can be comparable (smaller, larger or in the same order) depending on the type of the adsorbate, the interacting properties and the ratio of the thicknesses of the substrate and the film. The present theoretical framework quantifies the mechanisms of the adsorption-induced surface stress, and thus provides guidelines to the analysis of the sensitivities, and the identification of the detected substance in the design and application of micro- and nanocantilever sensors.

Acknowledgments

Yi and Duan acknowledge the financial support from the National Natural Science Foundation of China (under Grant nos. 10872003 and 10525209), the Foundation for the Author of National Excellent Doctoral Dissertation of China (FANEDD, under Grant no. 2007B2). Helpful discussions with Dr. Jörg Weissmüller of the Institute of Nanotechnology of Forschungszentrum Karlsruhe are also gratefully acknowledged.

Appendix A. Static deformation due to surface stress and eigenstrain

We assume that the cantilever is so slender ($T, L \gg h_f + h_s$) that it is accurate enough to use the Bernoulli–Euler beam theory. The strain in the cantilever can be decomposed into a uniform component and a bending component (Hsueh and Evans, 1985),

$$\varepsilon = c_0 + (z - h_b)K \quad (-h_s \le z \le h_f), \tag{A.1}$$

where c_0 is the uniform strain component, h_b denotes the position of the bending axis, and K is the curvature of the bending axis. It is noted that the bending axis is the line where the bending strain component is zero, whereas the conventional neutral axis is defined as the line where the total strain is zero.

The stresses σ_f and σ_s in the film and substrate can be obtained from Hooke's law,

$$\sigma_f = E_f(\varepsilon_f - \varepsilon^*), \quad \sigma_s = E_s\varepsilon_s, \tag{A.2}$$

where E is the Young modulus, and the subscripts f and s identify the quantities related to the film and substrate, respectively. In this paper, we use the one-dimensional model for simplicity, but the approach holds for the two-dimensional condition. If the two-layer structure is a plate rather than a cantilever, and $\varepsilon^*(z)$ is the in-plane biaxial eigenstrain, then E should be replaced by the biaxial modulus $E/(1-\nu)$, where ν is the Poisson ratio.

According to the equilibrium equations of the cantilever, i.e., the zero resultant forces ($\Sigma P_{c_0} = 0$ and $\Sigma P_b = 0$) due to the uniform strain and bending strain components, and the zero bending moment ($\Sigma M = 0$)

$$\Sigma P_{c_0} = \int_0^{h_f} E_f(c_0 - \varepsilon^*)\,dz + \int_{-h_s}^{0} E_s c_0\,dz + (a_u + a_l) + (b_u + b_l)c_0 - b_u\varepsilon^*(h_f), \tag{A.3}$$

$$\Sigma P_b = \int_0^{h_f} E_f(z - h_b)K\,dz + \int_{-h_s}^{0} E_s(z - h_b)K\,dz + b_u(h_f - h_b)K - b_l(h_s + h_b)K, \tag{A.4}$$

$$\Sigma M = \int_0^{h_f} \sigma_f(z - h_b)dz + \int_{-h_s}^{0} \sigma_s(z - h_b)dz + \tau_u(h_f - h_b) - \tau_l(h_s + h_b), \tag{A.5}$$

the uniform strain component c_0, the position of the bending axis h_b, and the curvature K can be obtained. The curvature K is given by Eqs. (23) and (24), and c_0 and h_b are given by

$$c_0 = \frac{E_f\int_0^{h_f}\varepsilon^*\,dz + b_u\varepsilon^*(h_f) - (a_u + a_l)}{\Gamma_3}, \tag{A.6}$$

$$h_b = \frac{E_f h_f^2 - E_s h_s^2 + 2h_f b_u - 2h_s b_l}{2\Gamma_3}, \tag{A.7}$$

where $\varepsilon^*(h_f)$ denotes the eigenstrain at the upper surface $z = h_f$. Note that the position of the bending axis is independent of the eigenstrain ε^* and constant surface stress a.

A.1. Curvature due to eigenstrain

Letting the surface stresses τ_u and τ_l in Eq. (23) vanish, the curvature induced by the eigenstrain $\varepsilon^*(z)$ is

$$K = \frac{6E_f[2(E_s h_s + E_f h_f)\int_0^{h_f} z\varepsilon^*\,dz + (E_s h_s^2 - E_f h_f^2)\int_0^{h_f}\varepsilon^*\,dz]}{h_f^4E_f^2 + h_s^4E_s^2 + 2E_fE_sh_fh_s(2h_s^2 + 3h_fh_s + 2h_f^2)}. \tag{A.8}$$

For a uniform eigenstrain (ε^* =const.), Eq. (A.8) becomes (Timoshenko, 1925; Freund, 1996)

$$K = \frac{6E_fE_sh_fh_s(h_f + h_s)\varepsilon^*}{h_f^4E_f^2 + h_s^4E_s^2 + 2E_fE_sh_fh_s(2h_s^2 + 3h_fh_s + 2h_f^2)}. \tag{A.9}$$

For $h_f \ll h_s$, Eq. (A.9) reduces to the Stoney formula in terms of ε^*, i.e., $K = 6E_fh_f\varepsilon^*/E_sh_s^2$.

A.2. Curvature due to surface stress

When $\varepsilon^*(z) = 0$, Eq. (23) reduces to

$$K = \frac{3c_0h_fh_b(E_f + E_s) + 3\Gamma_1}{6(h_s + h_b)^2b_l + 6(h_f - h_b)^2b_u + 2\Gamma_2}, \tag{A.10}$$

where Γ_1 and Γ_2 are given in Eq. (24) and

$$c_0 = -\frac{a_u + a_l}{\Gamma_3}, \quad h_b = \frac{E_f h_f^2 - E_s h_s^2 + 2h_f b_u - 2h_s b_l}{2\Gamma_3}. \tag{A.11}$$

If we only consider the strain-independent surface stresses a_u and a_l, the curvature described by Eq. (A.10) becomes

$$K = \frac{6[(a_l - a_u)(h_f^2 E_f + h_s^2 E_s) + 2h_f h_s(a_l E_f - a_u E_s)]}{h_f^4 E_f^2 + h_s^4 E_s^2 + 2E_f E_s h_f h_s(2h_s^2 + 3h_f h_s + 2h_f^2)}. \tag{A.12}$$

With $h_f \ll h_s$ and $b_u = b_l = 0$, the curvature in Eq. (A.12) reduces to the classical Stoney formula in terms of the surface stress a, i.e., $\Delta a = a_u - a_l = -E_s h_s^2 K/6$. The elimination of the bending curvature K from Eqs. (A.9) and (A.12) gives the equivalent relation between the uniform eigenstrain ε^* and the surface stress a, i.e.,

$$\varepsilon^* = \frac{(a_l - a_u)(h_f^2 E_f + h_s^2 E_s)}{E_f E_s(h_f + h_s)h_f h_s} + \frac{2(a_l E_f - a_u E_s)}{E_f E_s(h_f + h_s)}. \tag{A.13}$$

For $h_f \ll h_s$, Eq. (A.13) becomes $\Delta a = -E_f h_f \varepsilon^*$.

Appendix B. Resonance frequency due to adsorption mass and surface stress

We consider a two-layer cantilever subjected to the surface stress τ and the adsorption mass together. Neglecting the damping effect and shear deformation, the vibration equation of the cantilever loaded by a constant axial end force (F) is (Timoshenko et al., 1974)

$$-\frac{\partial^2 M}{\partial x^2} - F\frac{\partial^2 w}{\partial x^2} + (m + \Delta m)\frac{\partial^2 w}{\partial t^2} = 0, \tag{B.1}$$

where M is the bending moment, $m(= \rho_f A_f + \rho_s A_s)$, and Δm are the effective mass per unit length of the cantilever and mass loading, respectively (the mass of cantilever is $m_c = mL$, and the total mass loading is $\Delta m_t = \Delta mL$).

In the absence of external force ($F = 0$), Eq. (B.1) becomes

$$-\frac{\partial^2 M}{\partial x^2} + (m + \Delta m)\frac{\partial^2 w}{\partial t^2} = 0. \tag{B.2}$$

Using Eq. (A.5) and the relation $K = -\partial^2 w/\partial x^2$, the bending moment M on the cross-section of the two-layer cantilever is

$$\begin{aligned}\frac{M}{T} &= \int_0^{h_f} \sigma_f(z - h_b)\,dz + \int_{-h_s}^{0} \sigma_s(z - h_b)\,dz + \tau_u(h_f - h_b) - \tau_l(h_s + h_b) \\ &= -\left[(h_s + h_b)^2 b_l + (h_f - h_b)^2 b_u + \frac{1}{3}(E_f h_f^3 + E_s h_s^3) - E_f h_f h_b(h_f - h_b) + E_s h_s h_b(h_s + h_b)\right]\frac{\partial^2 w}{\partial x^2} - \Pi(\varepsilon^*, c_0, h_b),\end{aligned} \tag{B.3}$$

where h_b is given in Eq. (A.7), T is the width of the cantilever and $\Pi(\varepsilon^*, c_0, h_b)$ is a function of ε^*, c_0 and h_b. By substituting h_b by Eq. (A.7), Eq. (B.3) can also be expressed as

$$M = -TD'\frac{\partial^2 w}{\partial x^2} + \text{const.}, \tag{B.4}$$

where D' is given by Eq. (25).

In the case of $E_f = E_s = E$, Eq. (25) gives the expression of the bending stiffness of a homogeneous cantilever with the effect of the surface modulus,

$$D' = \frac{h^4 E^2 + 4Eh^3(b_u + b_l) + 12h^2 b_u b_l}{12(b_u + b_l + hE)}. \tag{B.5}$$

If the surface moduli of the upper and lower surfaces are equal, i.e. $b_u = b_l = b$, Eq. (B.5) reduces to the result ($D' = Eh^3/12 + bh^2/2$) given by Gurtin et al. (1976).

References

Berger, R., Delamarche, E., Lang, H.P., Gerber, C., Gimzewski, J.K., Meyer, E., Güntherodt, H.-J., 1997. Surface stress in the self-assembly of alkanethiols on gold. Science 276, 2021–2024.

Chakarova-Käck, S.D., Schröder, E., Lundqvist, B.I., Langreth, D.C., 2006. Application of van der Waals density functional to an extended system: adsorption of benzene and naphthalene on graphite. Phys. Rev. Lett. 96, 146107-1–146107-4.

Chen, G.Y., Thundat, T., Wachter, E.A., Warmack, R.J., 1995. Adsorption-induced surface stress and its effects on resonance frequency of microcantilevers. J. Appl. Phys. 77, 3618–3622.

Chun, D.W., Hwang, K.S., Eom, K., Lee, J.H., Cha, B.H., Lee, W.Y., Yoon, D.S., Kim, T.S., 2007. Detection of the Au thin-layer in the Hz per picogram regime based on the microcantilevers. Sensors Actuators A 135, 857–862.

Dareing, D.W., Thundat, T., 2005. Simulation of adsorption-induced stress of a microcantilever sensor. J. Appl. Phys. 97, 043526-1–043526-5.

Dorignac, J., Kalinowski, A., Erramilli, S., Mohanty, P., 2006. Dynamical response of nanomechanical oscillators in immiscible viscous fluid for in vitro biomolecular recognition. Phys. Rev. Lett. 96, 186105-1–186105-4.
Duan, H.L., Wang, J., Huang, Z.P., Karihaloo, B.L., 2005. Size-dependent effective elastic constants of solids containing nano-inhomogeneities with interface stress. J. Mech. Phys. Solids 53, 1574–1596.
Freund, L.B., 1996. Some elementary connections between curvature and mismatch strain in compositionally graded thin films. J. Mech. Phys. Solids 44, 723–736.
Godin, M., 2004. Surface stress, kinetics, and structure of alkanethiol self-assembled monolayers. Ph.D. Thesis, McGill University, Canada.
Grönbeck, H., Curioni, A., Andreoni, W., 2000. Thiols and disulfides on the Au(111) surface: the headgroup–gold interaction. J. Am. Chem. Soc. 122, 3839–3842.
Grossmann, A., Erley, W., Hannon, J.B., Ibach, H., 1996. Giant surface stress in heteroepitaxial films: invalidation of a classical rule in epitaxy. Phys. Rev. Lett. 77, 127–130.
Gurtin, M.E., Markenscoff, X., Thurston, R.N., 1976. Effect of surface stress on the natural frequency of thin crystals. Appl. Phys. Lett. 29, 529–530.
Gurtin, M.E., Murdoch, A.I., 1975. A continuum theory of elastic material surfaces. Arch. Ration. Mech. Anal. 57, 291–323.
Hsueh, C.H., Evans, A.G., 1985. Residual stresses in metal/ceramic bonded strips. J. Am. Ceram. Soc. 68, 241–248.
Huang, G.Y., Gao, W., Yu, S.W., 2006. Model for the adsorption-induced change in resonance frequency of a cantilever. Appl. Phys. Lett. 89, 043506-1–043506-3.
Huang, M., Rugheimer, P., Lagally, M.G., Liu, F., 2005. Bending of nanoscale ultrathin substrates by growth of strained thin films and islands. Phys. Rev. B 72, 085450-1–085450-6.
Hwang, K.S., Eom, K., Lee, J.H., Chun, D.W., Cha, B.H., Yoon, D.S., Kim, T.S., Park, J.H., 2006. Dominant surface stress driven by biomolecular interactions in the dynamical response of nanomechanical microcantilevers. Appl. Phys. Lett. 89, 173905-1–173905-3.
Ilic, B., Czaplewski, D., Craighead, H.G., Neuzil, P., Campagnolo, C., Batt, C., 2000. Mechanical resonant immunospecific biological detector. Appl. Phys. Lett. 77, 450–452.
Israelachvili, J.N., 1985. Intermolecular and Surface Forces: With Applications to Colloidal and Biological Systems. Academic Press, London.
Kohn, W., Lau, K.H., 1976. Adatom dipole moments on metals and their interactions. Solid State Commun. 18, 553–555.
Kramer, D., Viswanath, R.N., Weissmüller, J., 2004. Surface-stress induced macroscopic bending of nanoporous gold cantilevers. Nano Lett. 4, 793–796.
Lachut, M.J., Sader, J.E., 2007. Effect of surface stress on the stiffness of cantilever plates. Phys. Rev. Lett. 99, 206102-1–206102-4.
Lagowski, J., Gatos, H.C., Sproles, E.S., 1975. Surface stress and the normal mode of vibration of thin crystals: GaAs. Appl. Phys. Lett. 26, 493–495.
Lau, K.H., Kohn, W., 1977. Elastic interaction of two atoms adsorbed on a solid surface. Surf. Sci. 65, 607–618.
Li, X., Shih, W.Y., Aksay, I.A., Shih, W.-H., 1999. Electromechanical behavior of PZT-brass unimorphs. J. Am. Ceram. Soc. 82, 1733–1740.
Lu, P., Lee, H.P., Lu, C., O'Shea, S.J., 2005. Surface stress effects on the resonance properties of cantilever sensors. Phys. Rev. B 72, 085405-1–085405-5.
McFarland, A.W., Poggi, M.A., Doyle, M.J., Bottomley, L.A., Colton, J.S., 2005. Influence of surface stress on the resonance behavior of microcantilevers. Appl. Phys. Lett. 87, 053505-1–053505-3.
Nuzzo, R.G., Zegarski, B.R., Dubois, L.H., 1987. Fundamental studies of the chemisorption of organosulfur compounds on Au(111). Implications for molecular self-assembly on gold surfaces. J. Am. Chem. Soc. 109, 733–740.
Pala, R.G.S., Liu, F., 2004. Determining the adsorptive and catalytic properties of strained metal surfaces using adsorption-induced stress. J. Chem. Phys. 120, 7720–7724.
Park, H.S., Klein, P.A., 2008. Surface stress effects on the resonant properties of metal nanowires: the importance of finite deformation kinematics and the impact of the residual surface stress. J. Mech. Phys. Solids 56, 3144–3166.
Rappé, A.K., Casewit, C.J., Colewell, K.S., Goddard III, W.A., Skiff, W.M., 1992. UFF, a full periodic table force field for molecular mechanics and molecular dynamics simulations. J. Am. Chem. Soc. 114, 10024–10035.
Saya, D., Nicu, L., Guirardel, M., Tauran, Y., Bergaud, C., 2004. Mechanical effect of gold nanoparticles labeling used for biochemical sensor applications: a multimode analysis by means of SiN_x micromechanical cantilever and bridge mass detectors. Rev. Sci. Instrum. 75, 3010–3015.
Sony, P., Puschnig, P., Nabok, D., Ambrosch-Draxl, C., 2007. Importance of van der Waals interaction for organic molecule–metal junctions: adsorption of thiophene on Cu(110) as a prototype. Phys. Rev. Lett. 99, 176401-1–176401-4.
Stoney, G.G., 1909. The tension of metallic films deposited by electrolysis. Proc. R. Soc. A 82, 172–175.
Sun, Y.X., Fang, D.N., Soh, A.K., 2006. Thermoelastic damping in micro-beam resonators. Int. J. Solids Struct. 43, 3213–3229.
Timoshenko, S., 1925. Analysis of bi-metal thermostats. J. Opt. Soc. Am. 11, 233–255.
Timoshenko, S., Young, D.H., Weaver, W., 1974. Vibration Problems in Engineering, fourth ed. Wiley, New York.
Wu, G., Ji, H., Hansen, K., Thundat, T., Datar, R., Cote, R., Hagan, M.F., Chakraborty, A.K., Majumdar, A., 2001. Origin of nanomechanical cantilever motion generated from biomolecular interactions. Proc. Natl. Acad. Sci. USA 98, 1560–1564.
Yourdshahyan, Y., Rappe, A.M., 2002. Structure and energetics of alkanethiol adsorption on the Au(111) surface. J. Chem. Phys. 117, 825–833.
Zang, J., Huang, M., Liu, F., 2007. Mechanism for nanotube formation from self-bending nanofilms driven by atomic-scale surface-stress imbalance. Phys. Rev. Lett. 98, 146102-1–146102-4.
Zang, J., Liu, F., 2007. Theory of bending of Si nanocantilevers induced by molecular adsorption: a modified Stoney formula for the calibration of nanomechanochemical sensors. Nanotechnology 18, 405501-1–405501-4.
Zang, J., Liu, F., 2008. Modified Timoshenko formula for bending of ultrathin strained bilayer films. Appl. Phys. Lett. 92, 021905-1–021905-3.
Zhang, J.Q., Yu, S.W., Feng, X.Q., 2008. Theoretical analysis of resonance frequency change induced by adsorption. J. Phys. D Appl. Phys. 41, 125306-1–125306-8.